

# An Optimization Method for Multi-operator and Mixed-traffic LTE Deployments in the Unlicensed Bands

Abdel karim Ajami<sup>1</sup>, Hassan Artail<sup>1</sup>, Kang G. Shin<sup>2</sup>

<sup>1</sup>Electrical and Computer Engineering Department, American University of Beirut, Beirut, Lebanon

<sup>2</sup>Electrical Engineering and Computer Science Department, University of Michigan, Ann Arbor, USA

E-mails: <sup>1</sup>{asa72,ha27}@aub.edu.lb; <sup>2</sup>kgshin@umich.edu

**Abstract**—The proliferation of multimedia applications and services increased the demand on data and the requirement by operators to improve the experience of their users. This has motivated the extension of cellular technologies, such as Long Term Evolution (LTE) toward using the unlicensed bands. However, the nature of these bands poses a challenge since there is uncontrolled interference from other coexisting transmissions. We discuss in this paper the issue of efficient coexistence of LTE operators in the unlicensed bands through an optimization framework that is based on performance metrics obtained using stochastic geometry. The proposed optimization framework allows for obtaining optimized network topologies that maximize the benefit of LTE operators looking to deploy their networks in the unlicensed bands.

**Index Terms**—LTE, LAA, Stochastic Geometry, Unlicensed Band, Optimization, Network Planning, Co-existence.

## I. INTRODUCTION AND RELATED WORK

The fast development of web-enabled devices such as smart-phones along with social and multimedia services is pressuring network operators and device manufacturers throughout the world to look forward to increase the capacity of their cellular networks and upgrade it to the fifth generation (5G) [1]. The fundamental way to increase the capacity of the network is to utilize more bandwidth. However, the licensed spectrum is already very occupied, and hence, there is a need to seek alternative solutions. One solution is to utilize the unlicensed spectrum where the amount of available spectrum is comparable to or exceeds the amount of the licensed spectrum [2].

Initially, the unlicensed bands below 6 GHz, specifically those located around 2.4 GHz and 5 GHz, are considered. The 2.4 GHz ISM (Industrial, Scientific, and Medical) band is already crowded by a large number of devices and technologies. Hence, the 5 GHz bands were considered by LTE release 13 to address the potential coexistence with other legacy technologies such as WiFi. [3]. In this context, LTE was referred to as Licensed-Assisted Access (LAA) LTE. The LAA design should enable the fair coexistence between WiFi and LAA, and a fair coexistence between different LAA systems as well [4]. Several related regulations were foreseen by LTE release 13 [5], such as (i) Listen Before Talk (LBT) MAC-layer operations for fair coexistence with contention-based MAC protocols, and (ii) limitations on transmission power

(23/24 dBm in Europe/U.S. for indoor usage). The former feature is likely more important since in Europe and Japan the regulations for the utilization of the unlicensed bands require LBT. On the other hand, given that the latter feature makes LAA more suitable for indoor usage and that a major part of the traffic demand is generated indoors, LAA will undoubtedly play a key role in 5G [6].

Many research works have studied the coexistence of LTE and WiFi in the unlicensed bands, and discussed several LAA coexistence mechanisms. In addition to LBT [7], these include time and/or frequency domain based mechanisms (e.g., dynamic channel selection [8]), duty cycled transmissions [9], and power control [10]. Although these studies have shown that, while achieving fair coexistence with WiFi, LTE may be slightly affected by WiFi in some scenarios. Moreover, there may be significant performance degradations resulting from LAA inter-operator interference when deployed in the same area [11], [13].

This paper contributes to the fundamental understanding of the coexistence of LAA operators by using an optimization-based network planning framework that deals with efficient cell deployments. Although, the approach in [12] allows for computing optimized network topologies, it addresses only LTE-WiFi coexistence and is based on system level simulations. On the other hand, since the capacity limits of the coexisting LAA networks are still unclear, we develop in this paper a theoretical network planning and optimization framework. This framework is based on stochastic geometry, a tool that allows for capturing the spatial randomness and the physical layer characteristics using the signal-to-interference-plus-noise ratio (SINR) [16]–[18]. The use of this tool overcomes the limitations of the deterministic eNB topology and that of the Wyner model [14], where the former requires careful placement of cells resulting in large expenses for network providers while the latter is not accurate enough when modeling inter-cell interference [15].

We use the Newton-Raphson algorithm to efficiently assess the developed framework of LAA network topologies, where the input is the radio channel model, spatial location model, channel access model, and cost model. The output will be a set of optimized network topologies, where in our context,

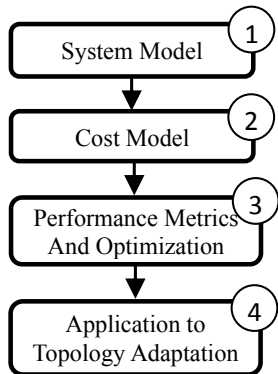


Fig. 1: Proposed Framework For LAA Network Deployment

optimization concerns the density of deployed base stations. In summary, the contributions of the paper are as follows:

- Contributing to the fundamental understanding of coexistence of LAA operators who may be using the same or different network configuration parameters and traffic services.
- Developing a theoretical network planning and optimization framework using stochastic geometry in contrast to other methods that use system-level simulations.
- Providing efficient assessment of LAA network topologies and determining the optimal density of deployed base stations to maximize performance or minimize cost.

## II. OPTIMIZATION FRAMEWORK

Our goal in this work is to determine the smallest number of eNBs necessary to satisfy a particular traffic demand. We do this by using a theoretical framework based on stochastic geometry in order to capture the performance resulting from the coexistence of different LAA networks.

### A. System Model

The mathematical framework we develop in this section allows for capturing the statistical performance of the coexisting networks. We describe the channel model, then the location model, and finally, the access model for LTE LAA.

1) *Radio Channel Model*: We denote by  $l(d)$  the path loss between the transmitter and the receiver which are separated by a distance  $d$ . We use here a common free space path loss model with reference distance of one meter for both LAA links. Hence,  $l(d) = \frac{\lambda_c \times d^\alpha}{4\pi}$  where  $\lambda_c$  represents the wavelength and  $\alpha$  is the path-loss exponent that depends on the scenario considered. Furthermore, we assume that channels are subject to i.i.d Rayleigh fading where each fading variable is exponentially distributed with parameter  $\mu$ .

2) *Spatial Location Model*: We consider mainly a scenario in which three operators coexist in a single unlicensed frequency band that has a bandwidth denoted by  $B$ . We assume that each of the operators use LTE-LAA, but may transmit different traffic types and may have different eNB densities. The LTE eNBs are assumed to be low power small

cell (pico-cell or femto-cell) eNBs. We model the location of eNBs having traffic for transmission and co-existing in the same band, as realizations of three independent homogeneous Poisson point processes (PPP)  $\Phi$  on  $\mathbb{R}^2$ . The LTE eNB process for each operator is assumed to have persistent downlink traffic, and hence, based on Slivnyak's theorem [19], we analyze the performance of a typical UE in the downlink that is assumed to be at the origin. Each UE is associated with its closest eNB, which provides the strongest average received power. Given that each of  $\Phi_A$ ,  $\Phi_B$ , and  $\Phi_C$  is a PPP with intensities  $\lambda_A$ ,  $\lambda_B$ , and  $\lambda_C$  respectively, the probability density function (PDF) of the distance from the typical UE to the tagged eNB in the downlink is  $f_R(r) = 2\pi r \lambda_X e^{-\lambda_X \pi r^2}$  where  $\lambda_X = \lambda_A, \lambda_B$  or  $\lambda_C$  accordingly.

3) *Channel Access Model of LTE-LAA*: We address a Load-Based Equipment (LBE) based MAC protocol in our analysis as in [20] [21]. In such a protocol, an LTE-LAA eNB performs clear channel assessment (CCA) procedure, where the channel is observed for at least  $20 \mu s$  (Channel Observation Time,  $COT$ ) to detect the presence of active transmitters for which the received signal power exceeds a certain detection threshold ( $T_L$ ). A channel is determined busy if the intending transmitter detects another LTE signal above  $T_L$ . If the channel is found idle, the LTE eNB can transmit, but if it is busy, the LTE eNB will then follow a random back-off period before transmission, selected randomly from a contention window in the interval  $[0; q] \times COT$ . The  $q$  parameter is selected in the range  $[4; 32]$  and determines the priority for an LTE-LAA device to access the medium. Throughout this study, we focus mainly on the scenario where we have three coexisting LTE-LAA networks for operators A, B, and C, each using a different  $q$  parameter  $q_A$ ,  $q_B$ , and  $q_C$  depending on the transmitted traffic type. We define the contender of an LTE eNB as the other LTE eNBs from which the received power at the former exceeds a threshold  $T_L$ , where  $T_{LA}$ ,  $T_{LB}$ , and  $T_{LC}$  correspond to the energy detection threshold of operators A, B, and C respectively. Each LTE eNB has an independent mark that represents the random back-off period, which is uniformly distributed in the interval  $[0; q]$ . The eNB is retained by the MAC protocol if it has a smaller timer (or back-off period) than all of its contenders. A medium access indicator is assigned to each LTE eNB, and is equal to one if the eNB is allowed to transmit by the corresponding MAC layer protocol, and zero otherwise.

### B. Cost Model

The total cost  $C_{tot,X}$ , including annual capital expenditure (CAPEX) and operational expenditure (OPEX), of the LAA network of operator X in area A is given by:

$$C_{tot,X} = \lambda_X C_X A \quad (1)$$

where  $\lambda_X A$  is the intensity of the LAA network of operator X in a total area A, while  $C_X$  is the total cost of one cell.

$$\begin{aligned}
& H_N(x_i, x_0, q_1, q_2, q_3, q_4, T_{L1}, T_{L4}/P_1, N_1, N_2, N_3, Q_1, Q_2, Q_3) = \\
& \frac{1}{q_1 \times q_4} \int_0^{q_1} \int_0^{q_4} \left(1 - \exp\left(-\mu \frac{T_{L4}}{P_1} l(\|x_i - x_0\|)\right)\right) \times \exp\left(-t' \left(\frac{N_1(x_i, T_{L1}, r_0)}{q_1} + \frac{N_2(x_i, T_{L1})}{q_2} + \frac{N_3(x_i, T_{L1})}{q_3}\right)\right) \\
& -t \left(\frac{N_1(x_0, T_{L1}, r_0)}{q_1} + \frac{N_2(x_0, T_{L1})}{q_2} + \frac{N_3(x_0, T_{L1})}{q_3}\right) + \min(t, t') \left(\frac{Q_1(x_i, x_0)}{q_1^2} + \frac{Q_2(x_i - x_0)}{q_2^2} + \frac{Q_3(x_i - x_0)}{q_3^2}\right) dt dt'
\end{aligned} \tag{2}$$

### C. Performance Metrics And Optimization

In this section, we define the performance metrics that are involved in the optimization problem. The main performance metric is the density of successful transmissions (DST) that depends on the medium access probability (MAP), and the SINR coverage probability derived in [13]. On the other hand, we define in Section III, the optimization problem and the adopted solution.

1) *Medium Access Probability*: The medium access probabilities of an LAA eNB for operators A, B, and C with contention window sizes  $[0; q_A]$ ,  $[0; q_B]$ , and  $[0; q_C]$  respectively, are given by:

$$\begin{aligned}
\mathbb{E}[e_0^A] &= \int_0^\infty \frac{1 - \exp(-K_A)}{K_A} f_{\|x_i\|}(r_0) dr_0 \\
\text{Where } K_A &= N_A(x_i, T_{LA}, r_0) + \frac{q_A}{q_B} N_B(x_i, T_{LA}) + \frac{q_A}{q_C} N_C(x_i, T_{LA}) \\
\mathbb{E}[e_0^B] &= \int_0^\infty \frac{1 - \exp(-K_B)}{K_B} f_{\|y_k\|}(r_0) dr_0 \\
\text{Where } K_B &= \frac{q_B}{q_A} N_A(y_k, T_{LB}) + N_B(y_k, T_{LB}, r_0) + \frac{q_B}{q_C} N_C(y_k, T_{LB}) \\
\mathbb{E}[e_0^C] &= \int_0^\infty \frac{1 - \exp(-K_C)}{K_C} f_{\|z_n\|}(r_0) dr_0 \\
\text{Where } K_C &= \frac{q_C}{q_A} N_A(z_n, T_{LC}) + \frac{q_C}{q_B} N_B(z_n, T_{LC}) + N_C(z_n, T_{LC}, r_0)
\end{aligned} \tag{3}$$

2) *SINR Coverage Probability*: Given that the tagged LAA eNB is located at  $x_0 = (r_0, 0)$ , the SINR coverage probability of the typical UE at the origin with SINR threshold  $T$  in the downlink is approximated as:

$$\begin{aligned}
& \hat{\mathbb{P}}_{SINR}^X(T, P_1, \lambda_1, \mathbb{P}_{MAP,1}, \lambda_2, \mathbb{P}_{MAP,2}, \lambda_3, \mathbb{P}_{MAP,3}) \\
& \approx \int_0^\infty \exp\left(-\mu T l(r_0) \frac{\sigma_N^2}{P_1}\right) \times \exp\left(-\int_{\mathbb{R}^2} \frac{Tl(r_0) \lambda_2 \mathbb{P}_{MAP,2}}{P_2} dx\right) \\
& \times \exp\left(-\int_{\mathbb{R}^2} \frac{Tl(r_0) \lambda_3 \mathbb{P}_{MAP,3}}{P_3} dx\right) \\
& \times \exp\left(-\int_{\mathbb{R}^2 \setminus B(0, r_0)} \frac{Tl(r_0) \lambda_1 \mathbb{P}_{MAP,1}}{l(\|x\|) + Tl(r_0)} dx\right) \times f_{\|x_0\|}(r_0) dr_0
\end{aligned}$$

Where  $\mathbb{P}_{MAP}^{1,2,3,4}(x, x_0) =$

$$\frac{H_N(x, x_0, q_1, q_2, q_3, q_4, T_{L1}, T_{L4}/P_1, N_1, N_2, N_3, Q_1, Q_2, Q_3)}{H_D(x_i, x_0, q_1, q_4, T_{L1}, P_4, N_1/q_1, N_2/q_2, N_3/q_3)} \tag{4}$$

And

$$\begin{aligned}
& H_D(x_i, x_0, q_1, q_4, T_{L1}, P_4, N_1/q_1, N_2/q_2, N_3/q_3) = \\
& \stackrel{(a)}{=} \frac{1}{q_1} \int_0^{q_1} \left(1 - \frac{t}{q_4} \exp\left(-\mu \frac{T_{L1}}{P_4} l(\|x_i - x_0\|)\right)\right) \\
& \times \exp\left[-\frac{t}{q_1} N_1(x_0, T_{L1}, r_0) - \frac{t}{q_2} N_2(x_0, T_{L1}) - \frac{t}{q_3} N_3(x_0, T_{L1})\right] dt
\end{aligned} \tag{5}$$

Note that  $H_N$  can be obtained using Eq. (2). Hence for operators A, B, and C, the SINR coverage probability of the typical UE is given by:

$$\begin{aligned}
& \hat{\mathbb{P}}_{SINR}^A(T, P_A, \lambda_A, \mathbb{P}_{MAP}^{A,B,C,A}(x, x_0), \lambda_B, \mathbb{P}_{MAP}^{A,B,C,B}(y, x_0), \lambda_C, \mathbb{P}_{MAP}^{A,B,C,C}(z, x_0)) \\
& \hat{\mathbb{P}}_{SINR}^B(T, P_B, \lambda_B, \mathbb{P}_{MAP}^{B,A,C,B}(y, y_0), \lambda_A, \mathbb{P}_{MAP}^{B,A,C,A}(x, y_0), \lambda_C, \mathbb{P}_{MAP}^{B,A,C,C}(z, y_0)) \\
& \hat{\mathbb{P}}_{SINR}^C(T, P_C, \lambda_C, \mathbb{P}_{MAP}^{C,A,B,C}(z, z_0), \lambda_B, \mathbb{P}_{MAP}^{C,A,B,B}(y, z_0), \lambda_A, \mathbb{P}_{MAP}^{C,A,B,A}(x, z_0))
\end{aligned} \tag{6}$$

where in general,  $N_X(y, T_L, r)$  can be calculated as:

$$\begin{aligned}
& N_X(y, T_{LX}, r) = \lambda_X \int_{\mathbb{R}^2 \setminus B(0, r)} \exp\left(-\mu \frac{T_{LX}}{P_X} l(\|x - y\|)\right) dx \\
& \text{Similarly, } Q_X(x_1, T_{L1}, x_2, T_{L2}, r) \text{ can be computed using:}
\end{aligned}$$

$$\begin{aligned}
& Q_X(z_1, T_{L1}, z_2, T_{L2}, r) = \\
& \lambda_X \int_{\mathbb{R}^2 \setminus B(0, r)} \exp\left(-\mu \frac{T_{L1}}{P_X} l(\|x - z_1\|) - \mu \frac{T_{L2}}{P_X} l(\|x - z_2\|)\right) dx \\
& \text{where } N_X(y, T_{LX}) = N_X(y, T_{LX}, 0) \text{ and } Q_X(z_1, z_2) = \\
& Q_X(z_1, T_{LX}, z_2, T_{LX}, r).
\end{aligned}$$

3) *Density of Successful Transmissions (DST)*: Given the decoding SINR requirement  $T$ , the DST is defined as the mean number of transmission links per unit area. We note that the LAA link is only activated when the tagged eNB accesses the channel, thus the DST for the LAA downlink is:

$$D_{suc}^X(\lambda_A, \lambda_B, \lambda_C, T) = \lambda_X \mathbb{E}[e_0^X] \mathbb{P}(SINR_0^X > T | e_0^X = 1) \tag{7}$$

Based on that, we define the normalized DST as the probability to have a successful transmission link, as follows:

$$d_{suc}^X(\lambda_A, \lambda_B, \lambda_C, T) = \mathbb{E}[e_0^X] \mathbb{P}(SINR_0^X > T | e_0^X = 1) \tag{8}$$

### D. Application to Topology Adaptation

The optimized eNB densities resulting from optimization may be used either for planning LAA deployments, or with the Cloud-Radio Access Network (C-RAN) framework [22] to perform real-time cell switch-offs [23].

## III. OPTIMIZATION PROBLEM FORMULATION AND ADOPTED SOLUTION

Given a particular traffic type (voice, video, best effort, etc.), we investigate first the scenario where the operator would like

---

**Algorithm 1** Finding optimal operator density
 

---

**require**
*Density of eNBs for other coexisting operators*
*Initial density of operator X:  $\lambda_{X_0}$* 
*Maximum number of iterations:  $N_{Iter}$* 
*Define tolerance margin:  $\epsilon$* 
*Outage probability:  $P_{out}$  // for (10)*
**procedure** COMPUTE OPTIMAL  $\lambda_X$ 
 $\lambda_{X_n} \leftarrow \lambda_{X_0}$ 
**while** ( $N_{Iter} > 0$ ) **do**

$$f'(\lambda_{X_n}) \leftarrow \left. \frac{\partial}{\partial \lambda_X} (d_{suc}^X(\lambda_A, \lambda_B, \lambda_C, T_{min})) \right|_{\lambda_X = \lambda_{X_n}}$$

$$f''(\lambda_{X_n}) \leftarrow \left. \frac{\partial^2}{\partial \lambda_X^2} (d_{suc}^X(\lambda_A, \lambda_B, \lambda_C, T_{min})) \right|_{\lambda_X = \lambda_{X_n}}$$

$$\lambda_{X_{n+1}} \leftarrow \lambda_{X_n} - \frac{f'(\lambda_{X_n})}{f''(\lambda_{X_n})}$$

$$P \leftarrow \left. d_{suc}^X(\lambda_A, \lambda_B, \lambda_C, T_{min}) \right|_{\lambda_X = \lambda_{X_{n+1}}}$$

*// To calculate optimal  $\lambda_X$  for (9)*
**if** ( $\lambda_{X_{n+1}} - \lambda_{X_n} < \epsilon$ ) **then**
 $\lambda_{X_{optimal}} \leftarrow \lambda_{X_{n+1}}$ 
*Optimal normalized DST  $\leftarrow P$  return*
**else**
 $\lambda_{X_n} \leftarrow \lambda_{X_{n+1}}$ 
 $N_{Iter} \leftarrow N_{Iter} - 1$  **continue**
**end if**
*// To calculate optimal  $\lambda_X$  for (10)*
**if**  $P \geq (1 - P_{out})$  **then**
 $\lambda_{X_{optimal}} \leftarrow \lambda_{X_{n+1}}$ 
 $C_{tot,X} \leftarrow \lambda_{X_{optimal}} \times C_{eNB}$  **return**
**else**
 $\lambda_{X_n} \leftarrow \lambda_{X_{n+1}}$ 
 $N_{Iter} \leftarrow N_{Iter} - 1$  **continue**
**end if**
**end while**
**end procedure**


---

to optimize the performance and has no constraints on the cost. This allows for understanding the optimal performance that can be achieved by different operators using optimal eNB densities for various traffic scenarios. Hence, given the minimum SINR decoding requirement  $T_{min}$ , this can be formulated as follows:

$$\begin{aligned} \max \quad & d_{suc}^X(\lambda_A, \lambda_B, \lambda_C, T) \\ \text{s.t.} \quad & T \geq T_{min} \end{aligned} \quad (9)$$

Then, we consider minimizing the cost for an LAA operator to provide a particular outage probability  $P_{out}$  as follows:

$$\begin{aligned} \min \quad & C_{tot,X} \\ \text{s.t.} \quad & d_{suc}^X(\lambda_A, \lambda_B, \lambda_C, T) \geq \lambda_X(1 - P_{out}) \end{aligned}$$

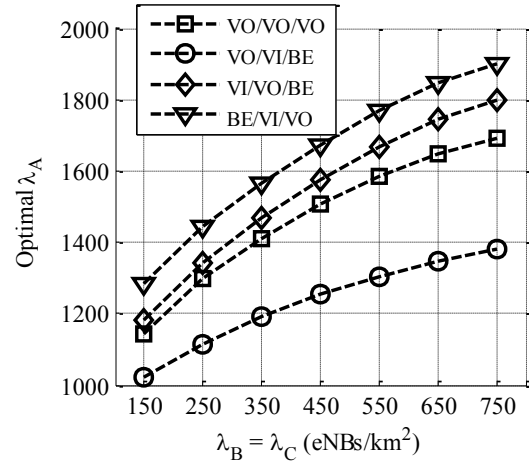


Fig. 2: Optimal  $\lambda_A$  that maximize the normalized DST of operator A under different traffic scenarios.

$$\& T \geq T_{min} \quad (10)$$

Since the function  $d_{suc}^X(\lambda_A, \lambda_B, \lambda_C, T_{min})$  is nonlinear, we apply the practical and effective global optimization Newton-Raphson technique [24] to find the optimal eNB densities  $\lambda_{X_{optimal}}$  that provide maximum performance  $P_{optimal}$  and minimum total deployment cost for operator X, as in (9) and (10) respectively.

#### IV. OPTIMIZATION RESULTS

Here, we utilize the developed optimization framework to compute statistically optimized network topologies that maximize the performance of a particular operator or minimize the deployment cost under outage probability constraints. We consider three coexisting LAA operators A, B, and C. Moreover, we focus on a dense network deployment where we vary the type of traffic transmitted by an operator, to show the effect of eNB densities and traffic types on the optimal performance or on the total deployment cost. The following contention window parameters,  $q_X = 3, 7,$  and  $15$  have been used for voice (VO), video (VI), and best effort (BE) traffic respectively, based on [25]. The Rayleigh fading parameter  $\mu$  is equal to 1, and we assume that the noise power is negligible as compared to the interference power ( $\sigma_N^2 = 0$ ). In addition, we consider for demonstration a minimum decoding SINR requirement  $T_{min} = -2.6$  dB for a QPSK modulation with a coding rate of  $1/8$ , according to [26].

We start by analyzing the impact of operator coexistence on the optimal densities of eNBs. That is, we initially consider the optimization problem in (9), where an operator wants to maximize his density of successful transmissions, given a minimum SINR requirement and that there are no constraints on the deployment cost.

Fig. 2 shows the computed optimal eNB densities  $\lambda_A$  for operator A versus the variation of densities  $\lambda_B$  and  $\lambda_C$  of operators B and C, respectively, while considering different traffic scenarios. Since we focus on the effect of the variation of the

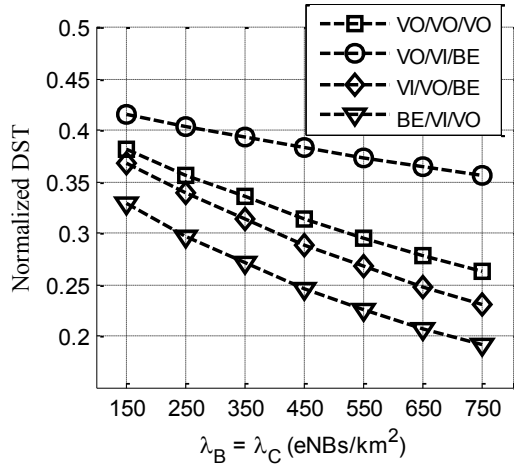


Fig. 3: Optimal normalized DST of operator A under different traffic scenarios.

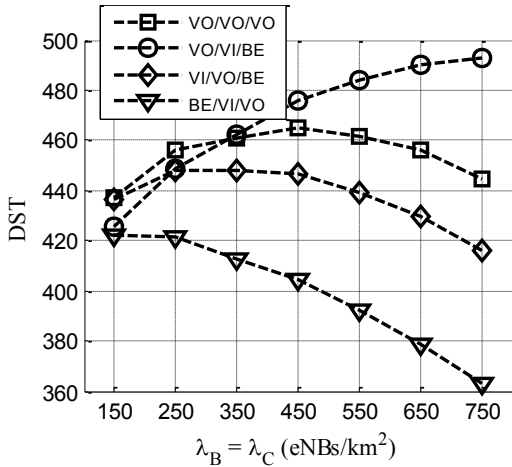


Fig. 4: Optimal DST of operator A under different traffic scenarios.

eNB densities and traffic types per operator, we adopted the energy detection thresholds  $T_{LA} = T_{LB} = T_{LC} = -72$  dBm and the eNB transmission power  $P_A = P_B = P_C = 23$  dBm. The figure illustrates that when  $\lambda_B = \lambda_C = 150$  eNBs/km<sup>2</sup>, the optimal  $\lambda_A$  that maximizes the normalized DST in case of all operators having voice traffic (VO/VO/VO) is 1140 eNBs/km<sup>2</sup>, which is relatively large as compared to 150 eNBs/km<sup>2</sup>. However, this corresponds to the density of eNBs that allows operator A to utilize the maximum capacity available in the channel, which is demonstrated in Fig. 3 that plots the normalized DST corresponding to the optimal  $\lambda_A$  values in Fig. 2. For example, in the case of VO/VO/VO scenario, the normalized DST is 0.38 for ( $\lambda_A = 1140$  eNBs/km<sup>2</sup>,  $\lambda_B = 150$  eNBs/km<sup>2</sup>,  $\lambda_C = 150$  eNBs/km<sup>2</sup>). That is, operator A has to deploy  $\lambda_A = 1140$  eNBs/km<sup>2</sup> in order to achieve a maximum of 433 successful transmission links per km<sup>2</sup> with a minimum decoding SINR requirement  $T_{min} = -2.6$  dB

as described earlier. We note that while the optimal  $\lambda_A$  that is required for operator A to achieve maximum performance increases for a particular traffic scenario as the densities of the coexisting operators  $\lambda_B$  and  $\lambda_C$  increase (from Fig. 2), Fig. 3 shows that when  $\lambda_B$  and  $\lambda_C$  increase, the maximum normalized DST that can be achieved decreases.

Also, by analyzing Fig. 2, we can see that the minimum optimal  $\lambda_A$  for different  $\lambda_B$  and  $\lambda_C$  values exists in the case of VO/VI/BE (i.e., operator A has voice traffic). In this case, based on the contention window parameters described earlier, the voice traffic will have higher priority than video (VI) and best effort (BE) traffic. This leads to savings in the deployment cost for operator A, as compared to other traffic scenarios. On the other hand, the optimal  $\lambda_A$  increases in case of VO/VO/VO (same traffic type across operators) for different  $\lambda_B$  and  $\lambda_C$  values, and it is higher in case where operator A has a traffic type with a lower priority than that of the other operators (VI/VO/BE or BE/VI/VO scenario).

From a different perspective, Fig. 3 shows that traffic scenarios where operator A has higher priority traffic, e.g. VO/VI/BE, the resulting normalized DST is the highest, although a lower optimal  $\lambda_A$  is required as compared to other traffic scenarios. The normalized DST starts to decrease as the priority of traffic carried by operator A is equal to or less than that of operators B and C.

Finally, we show in Fig. 4 the density of successful transmissions (DST) defined as the product of the optimal density of eNBs  $\lambda_A$  and the normalized DST, shown in Figs. 2 and 3, respectively, computed for every ( $\lambda_B, \lambda_C$ ) value. By inspecting Fig. 4, we can realize that there are three interesting trends. The first one is for the BE/VI/VO traffic where we see that as  $\lambda_B$  and  $\lambda_C$  increase, the optimal DST of operator A starts to decrease rapidly, although a higher density of eNBs  $\lambda_A$  is being used as shown in Fig. 2. Using a similar analysis, the second trend appears in case of VO/VO/VO and VI/VO/BE, where the DST increases until it reaches a maximum value, then starts decreasing even though a higher density of eNBs  $\lambda_A$  is utilized, as shown in Fig. 2. Finally, the third interesting trend appears in case of the VO/VI/BE traffic scenario where we observe that as  $\lambda_B$  and  $\lambda_C$  increase, the DST keeps on increasing. In this scenario, as the operator is investing in installing additional eNBs, better performance is achieved, which is not the case in the other traffic scenarios.

Next, we consider the optimization problem in (10) where an operator is looking to minimize the deployment cost (or number of deployed eNBs), subject to a minimum decoding SINR requirement and outage probability constraint  $P_{out}$ . In this problem, the operator is looking to deploy the minimal density of eNBs that satisfies his  $P_{out}$  requirement. As Fig. 3 illustrates, the normalized DST has a maximum value of 0.42 in case of VO/VI/BE traffic, corresponding to a minimum  $P_{out} =$  that is equal to 0.58. Similar calculations can be done for the other traffic types, and so, we plot the minimum densities  $\lambda_A$  required to satisfy  $P_{out}$ , as shown in Fig. 5, where  $\lambda_B = \lambda_C = 150$  eNBs/km<sup>2</sup>. By analyzing this

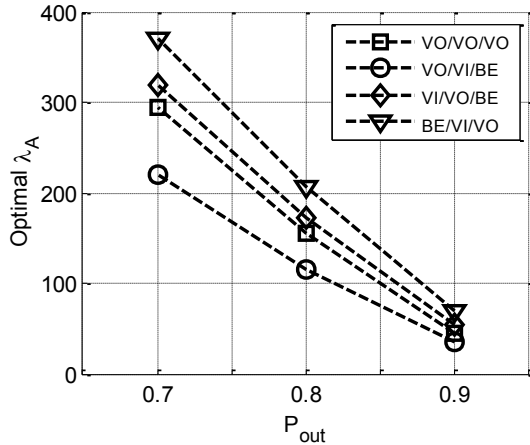


Fig. 5: Optimal  $\lambda_A$  required to provide  $P_{out}$  for operator A under different traffic scenarios.

figure, we see that for large  $P_{out} = 0.9$ , the optimal  $\lambda_A$  needed to satisfy this  $P_{out}$  constraint is quite similar for all traffic scenarios. However, as  $P_{out}$  decreases (and hence the need for more coverage increases), the operators will require more eNBs, where the difference between the optimal  $\lambda_A$  required by different traffic scenarios becomes significant. For example, by comparing the VO/VI/BE and the BE/VI/VO, we observe that operator A can save about 150 eNBs/km<sup>2</sup> in the VO/VI/BE scenario, as compared to the BE/VI/VO scenario for  $P_{out} = 0.7$ . This has a direct and significant impact on the total deployment cost.

## V. CONCLUSION

In this paper, we presented and validated an optimization framework based on stochastic geometry that allows an operator to plan his deployment in case of three different coexisting LAA networks in the unlicensed band. The developed framework allows the operator to compute optimized eNB densities in order to maximize the performance, or minimize the deployment cost under desired outage probability constraints. Throughout the analysis, we used the density of successful transmissions as a performance metric. Results show the effect of the variation of eNBs and traffic types used by the operators on the computed optimal density of eNBs. In addition, the maximum capacity of the channel was presented along with the minimum eNBs required for a target outage probability where we showed the impact of traffic scenarios on the deployment cost in terms of the extra number of eNBs needed. In the future, this work can be extended by assuming non-full buffer downlink traffic and by extending the number of coexisting operators for more than three.

## ACKNOWLEDGMENT

The authors acknowledge the generous support from the Lebanese National Council for Scientific Research (CNRS), under Project no. 22911, Award no. 103062.

## REFERENCES

- [1] UMTS Forum Mobile Traffic Forecasts 2010-2020.
- [2] Huawei white paper: U-LTE: Unlicensed Spectrum Utilization of LTE, 2014.
- [3] 3GPP RP-140808, "Review of regulatory requirements for unlicensed spectrum," June 2014.
- [4] 3GPP TR 36.889, "Study on licensed-assisted access to unlicensed spectrum," 2015.
- [5] R. Zhang, M. Wang, L. X. Cai, Z. Zheng, X. Shen, L. Xie, "LTE Unlicensed: The future of spectrum aggregation for cellular networks," *IEEE Wireless Communications Magazine*, IEEE Wireless Communications, Vol. 22, No.3, pp. 150-159, June 2015.
- [6] A. Osseiran et al, "Scenarios for 5G mobile and wireless communications: the vision of the METIS project," in *IEEE Communications Magazine*, vol. 52, no. 5, pp. 26-35, May 2014.
- [7] H. Ko, J. Lee, and S. Pack, "A fair listen-before-talk algorithm for coexistence of LTE-U and WLAN," *IEEE Transactions on Vehicular Technology*, vol. PP, no. 99, pp. 11, 2016.
- [8] O. Sallent et al, "Learning-based coexistence for LTE operation in unlicensed bands," in *Proc. 2015 IEEE International Conference on Communication Wksp. (ICCW)*, June 2015, pp. 23072313.
- [9] R. Zhang, M. Wang, L. Cai, Z. Zheng, and X. Shen, "LTE-unlicensed: the future of spectrum aggregation for cellular networks," *IEEE Wireless Communications*, vol. 22, no. 3, pp. 150159, Jun. 2015.
- [10] F. Chaves et al, "LTE UL power control for the improvement of LTE/Wi-Fi coexistence," in *Proc. IEEE 78th Vehicular Technology Conference (VTC 2013 Fall)*, Sept 2013, pp. 16.
- [11] M. D. Foegelle, "Coexistence of LTE-U and LAA in a Wi-Fi world," 2016 10th European Conference on Antennas and Propagation (EuCAP), Davos, 2016, pp. 1-5.
- [12] O. Sandoval, G. David Gonzalez, J. Hmlinen and S. Yoo, "Indoor planning and optimization of LTE-U radio access over WiFi," *2016 IEEE 27th Annual International Symposium on Personal, Indoor, and Mobile Radio Communications (PIMRC)*, Valencia, 2016, pp. 1-7.
- [13] A. k. Ajami and H. Artail, "Fairness in future Licensed Assisted Access (LAA) LTE networks: What happens when operators have different channel access priorities?," *2017 ICCW*, Paris, France, 2017, pp. 67-72.
- [14] A. D. Wyner, "Shannon-Theoretic Approach to a Gaussian Cellular Multiple-Access Channel", in *IEEE Trans. Inf. Theory*, vol. 40, no. 11, pp. 1713-1727, Nov. 1994.
- [15] Xu JiaMing et Al., "On the Accuracy of the Wyner Model in Cellular Networks", in *IEEE Trans. Wireless Commun.*, vol. 10, no. 9, pp. 3098-3109, Sep. 2011.
- [16] A. Borkar, C. Ibars, and P. Zong, "On the throughput analysis of LTE and WiFi in unlicensed band," in *Asilomar Conference on Signals, Systems and Computers*, pp. 1309-1313, Nov. 2014.
- [17] Y. Li, F. Baccelli, et Al., "Modeling and Analyzing the Coexistence of Wi-Fi and LTE in Unlicensed Spectrum," in *IEEE Transactions on Wireless Communications*, vol. 15, no. 9, pp. 6310-6326, Sept. 2016.
- [18] A. k. Ajami and H. Artail, "On The Modeling and Analysis of Uplink and Downlink IEEE 802.11ax Wi-Fi with LTE in Unlicensed Spectrum," in *IEEE Transactions on Wireless Communications*, 2017. DOI: 10.1109/TWC.2017.2715834.
- [19] S. N. Chiu, D. Stoyan, W. Kendall, and J. Mecke, *Stochastic geometry and its applications*. John Wiley & Sons, 2013.
- [20] C. Casetti, "Coexistence of IEEE 802.11n and licensed-assisted access devices using listen-before-talk techniques," 2016 13th IEEE Annual Consumer Communications & Networking Conference (CCNC), Las Vegas, NV, 2016, pp. 562-567.
- [21] ETSI EN 301.893 v1.7.1. "Broadband Radio Access Networks (BRAN); 5 GHz high performance RLAN."
- [22] J. Wu, Z. Zhang, Y. Hong, and Y. Wen, "Cloud radio access network (C-RAN): a primer," *IEEE Network*, vol. 29, no. 1, pp. 35-41, Jan 2015.
- [23] D. Gonzalez G., H. Yanikomeroglu, M. Garcia-Lozano, and S. R. Boque, "A novel multi-objective framework for cell switch-off in dense cellular networks," in *IEEE Int. Conference on Communications (ICC)*, June 2014, pp. 2641-2647.
- [24] J. H. Mathews, K. K. Fink, "Numerical Methods Using Matlab", Pearson, 4th Edition, 2004.
- [25] 3GPP TS 36.213, Technical specification group radio access network; Physical Layer Procedures (Release 14).
- [26] S. Sesia, I. Toufik, M. Baker, "LTE the UMTS Long Term Evolution From Theory to Practice", Wiley, 2nd Edition, 2011.